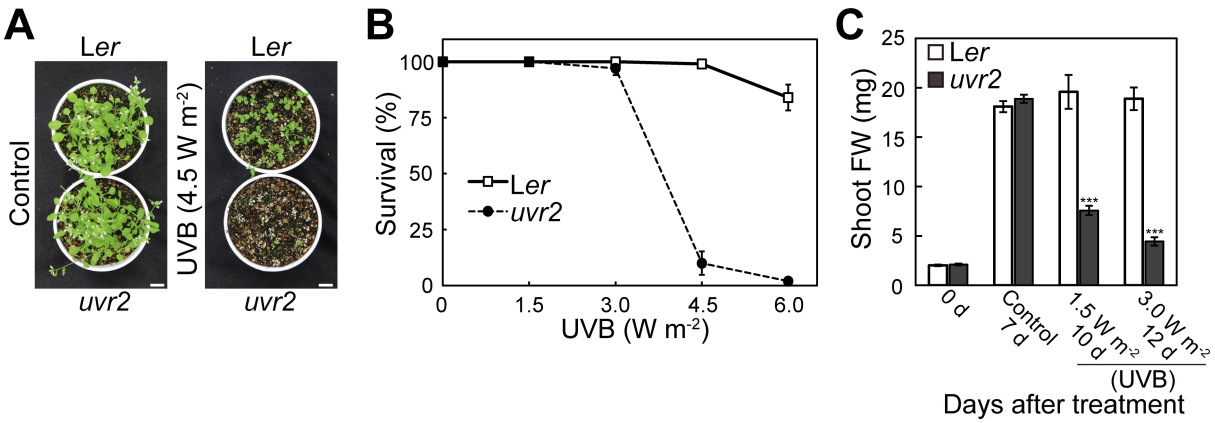

Supplemental Figure 1. Sensitivity of *uvr2* mutant plants to UVB-induced damage.
(A) Phenotypes of seedlings of wild-type ecotype Landsberg *erecta* (L*er*) and *uvr2* plants 10 d after a 1-h UVB exposure of 11 d-old seedlings at 4.5 W m^{-2}.Control indicates untreated, 21 d-old plants. Bars = 10 mm.
(B) and **(C)** The survival **(B)** and shoot fresh weight of indicated seedlings **(C)** after a 1-h UVB treatment at 1.5 to 6.0 W m^{-2}, based on experiments described in **(A)** (**[B],** ±SE., *n* = 3 or 5; **[C]**, ±SE, *n* = 8). Asterisks denote significant differences between genotypes based on a *t* test (***P< 0.001).

(Supports Figure 1.)

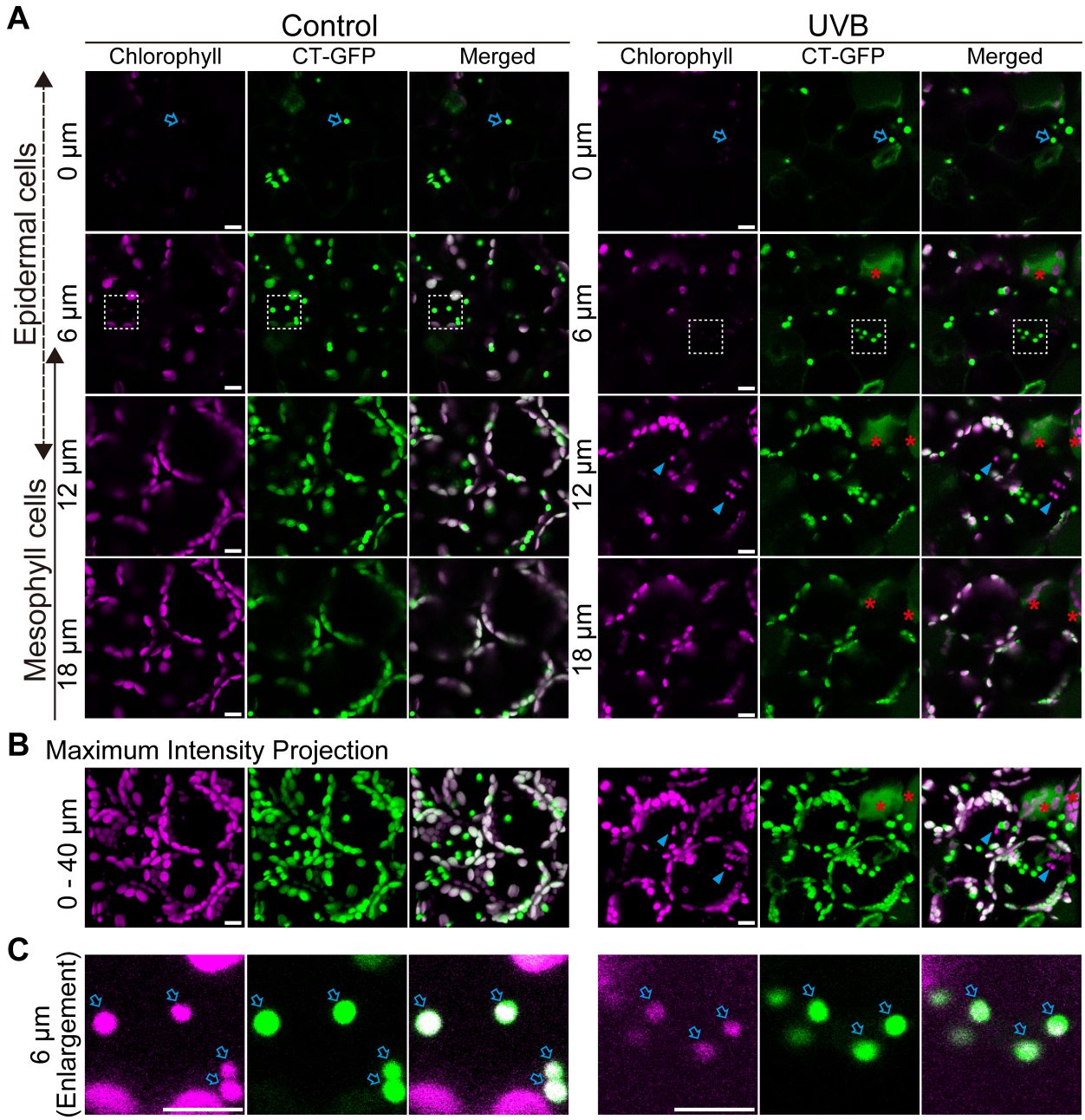

Supplemental Figure 2. 3-D observation of the appearance of CT-GFP-deficient chloroplasts in leaves of *Pro35S:CT-GFP* plants.

3-D observation of leaves expressing stromal CT-GFP from untreated control plants or plants exposed to UVB (1.5 W m^{-2}) for 2 h. Images were taken 2 d after treatment. The 40 µm-depth regionss from the top of epidermal cells were continuously observed, and the images were obtained at 1-µm resolution. The images at 0, 6, 12 and 18 µm from the top **(A)**, and the maximum intensity projection imaged from all images **(B)** are shown. The region indicated by squares in the images at 6 µm from the top, which include epidermal chloroplasts, are shown with enhanced fluorescence intensity **(C)**. Arrows indicate typical chloroplasts in epidermal cells, which contain faint chlorophyll auto-fluorescence and strong CT-GFP. Such chloroplasts were observed in both control and UVB-exposed leaves. In UVB-exposed leaves, CT-GFP-deficient chloroplasts (arrowheads) and dead cells (asterisks) were observed. Scale bars = 10 µm. For the evaluation of the frequency of CT-GFP-deficient chloroplasts, we observed larger regions (212 × 212 × 40 µm) and measured the proportion of cells with CT-GFP-deficient chloroplasts within all mesophyll cells.

(Supports Figure 2.)

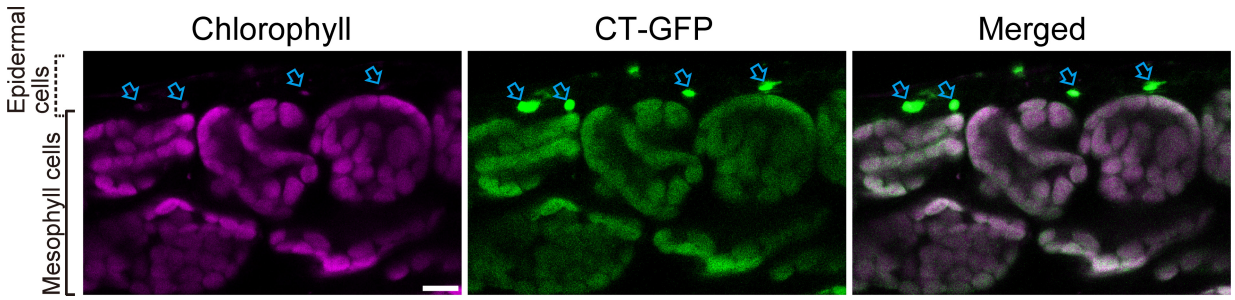

Supplemental Figure 3. Chloroplasts exhibiting strong CT-GFP and faint chlorophyll are located in epidermal cells.
Confocal images of a cross-section from leaves expressing stromal CT-GFP. Chlorophyll appears magenta and stromal CT-GFP appears green. Scale bar = 10 μm. Arrows indicate epidermal chloroplasts exhibiting strong CT-GFP and faint chlorophyll signals.

(Supports Figure 2.)

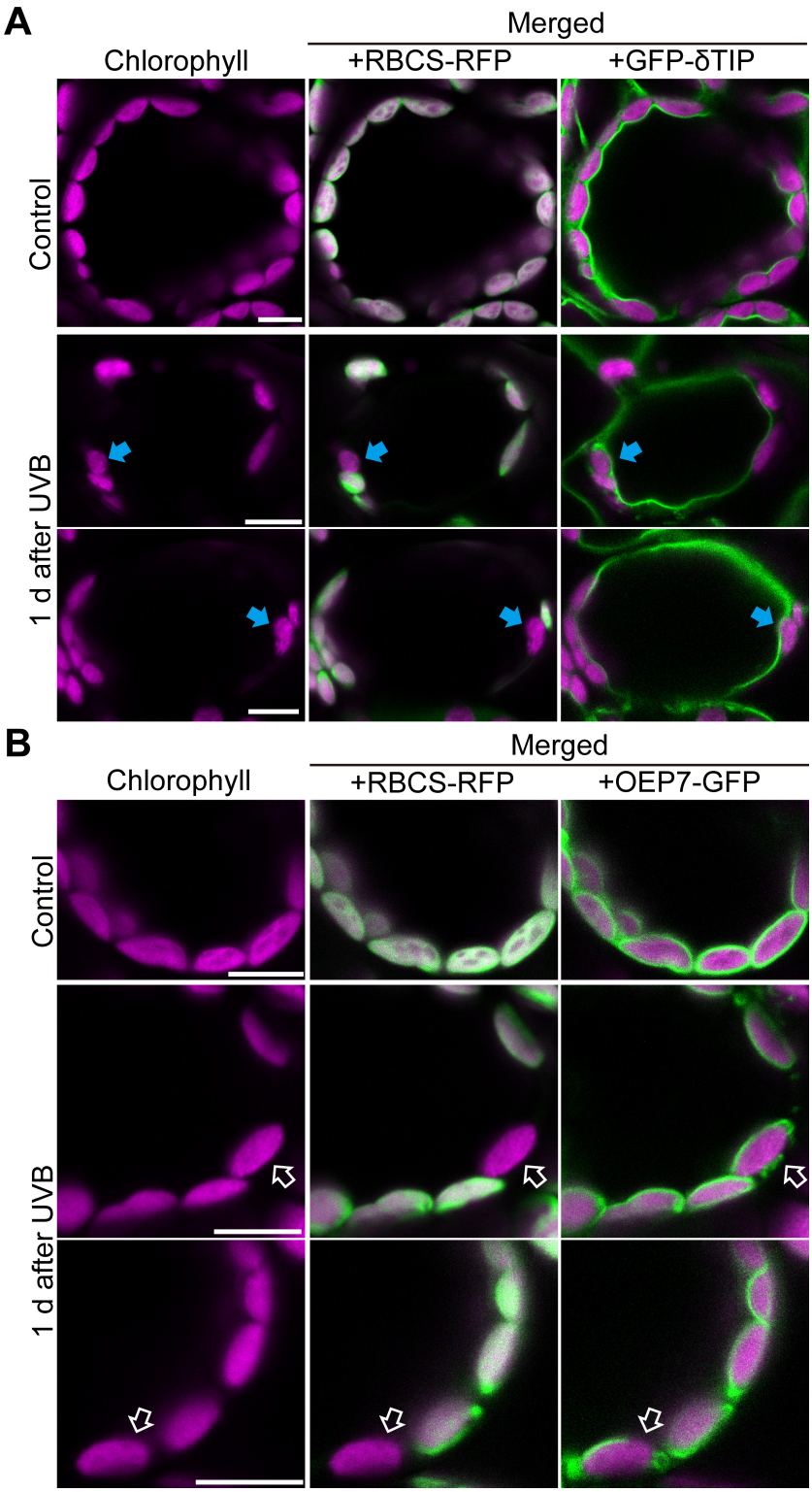

Supplemental Figure 4. Cytosolic collapsed chloroplasts exhibit damaged envelopes.
(A) Confocal images of leaf mesophyll cells expressing stromal RBCS-RFP and tonoplast GFP-δTIP from untreated control plants or plants exposed to UVB (1.5 W m^{-2}) for 2 h. Images were taken 1 d after treatment. Closed arrows indicate cytosolic chloroplasts lacking stromal RBCS-RFP, which were localized outside the GFP-δTIP-labeled tonoplast.
(B) Confocal images of leaf mesophyll cells expressing stromal RBCS-RFP and chloroplast envelope OEP7-GFP from untreated control plants or plants exposed to UVB for 2 h. Images were taken 1 d after treatment. Open arrowheads indicate RBCS-RFP-deficient chloroplasts in the cytoplasm, which were localized outside the GFP-δTIP-labeled tonoplast (arrowheads). Arrows indicate cytosolic chloroplasts lacking stromal RBCS-RFP exhibiting aberrant OEP7-GFP-labeled envelopes.

(Supports Figure 4.)

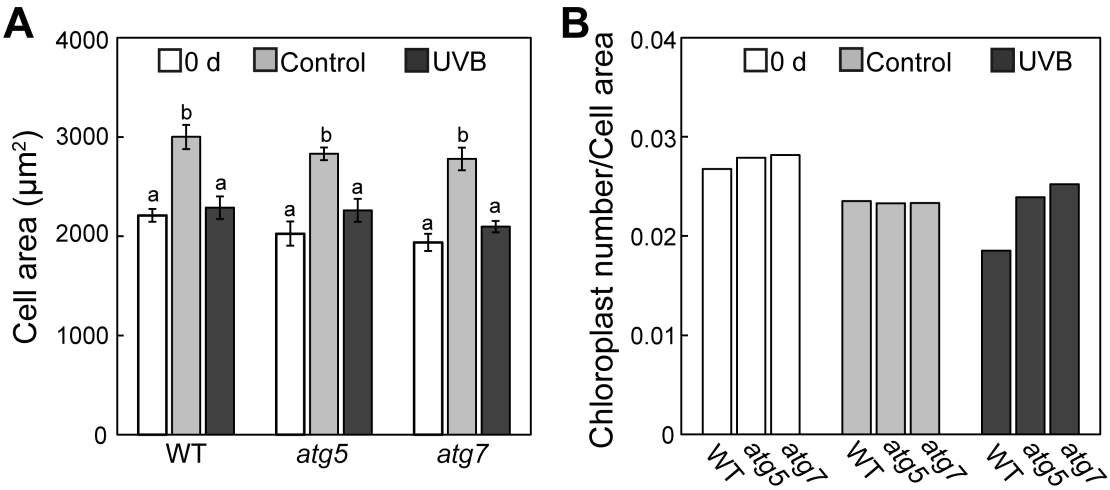

Supplemental Figure 5. Mesophyll cell area does not decrease due to UVB exposure.
(A) The planar area of fixed mesophyll cells from leaves before treatment (0 d), from untreated leaves as controls or from 2-h UVB (1.5 W m^{-2}) exposed leaves 3 d after treatment in WT, *atg5* and *atg7* plants (±SE, *n* = 10-16). The representative images are shown in Figure 5A. Different letters denote significant difference from each other based on Tukey's test ($P < 0.05$).
(B) The ratio of chloroplast number to mesophyll cell area from the data described in **(A)** and Figure 5B.

(Supports Figure 5.)

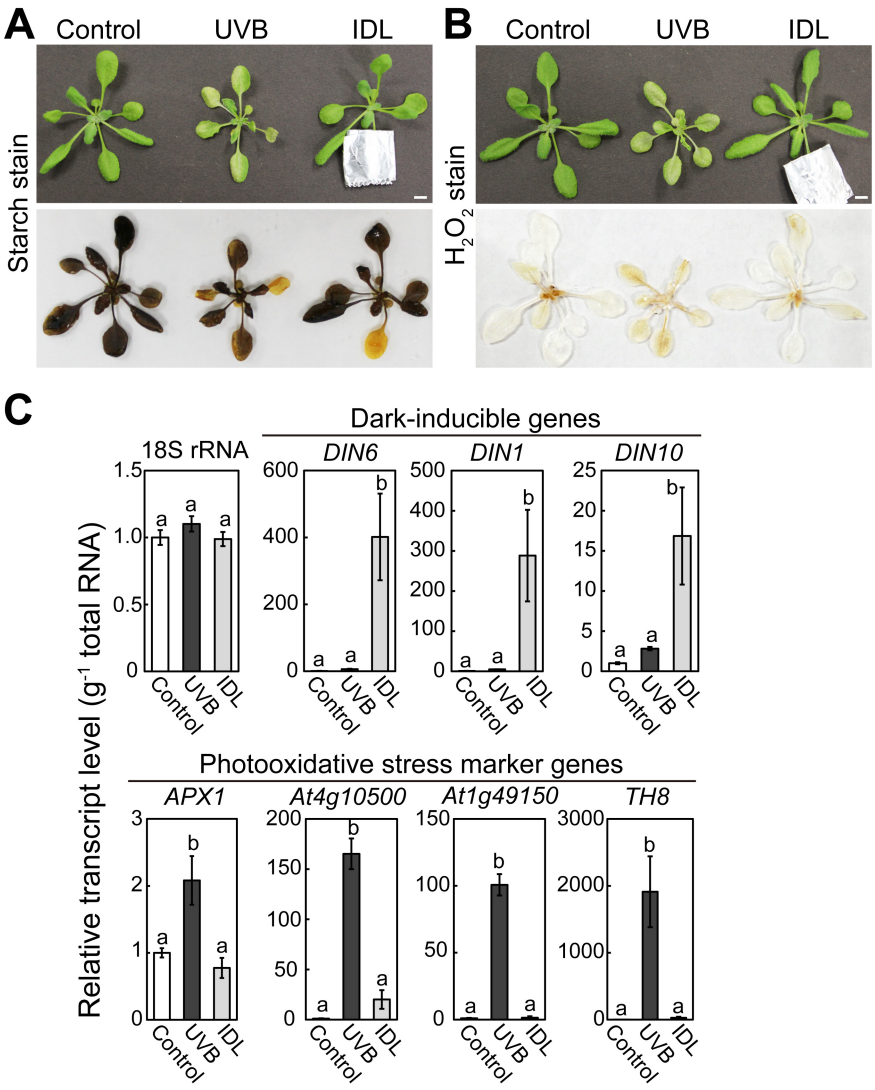

Supplemental Figure 6. Comparison of phenotypes between individually darkened leaves (IDLs) and UVB-exposed leaves.

(A) and **(B)** Iodine staining of starch **(A)** or DAB staining of H_2O_2 **(B)** in untreated plants as controls, in plants at 3 d IDL treatment or plants 3 d after 2-h UVB treatment at 1.5 W m^{-2}. Scale bars = 10 mm.

(C) Transcripts for dark-inducible genes and photooxidative-stress marker genes in leaves of untreated control plants, in leaves at 3 d IDL treatment or leaves 3 d after a 2-h UVB treatment (1.5 W m^{-2}). Transcript levels of three dark-inducible genes and four photooxidative stress marker genes were analyzed by qRT-PCR (±SE, *n* = 3-4). Transcript levels of respective genes are shown relative to the values from control leaves, which are set to 1. The level of 18S rRNA was measured as an internal standard. Different letters in each graph denote significant difference from each other based on Tukey's test ($P < 0.05$).

(Supports Figure 9.)

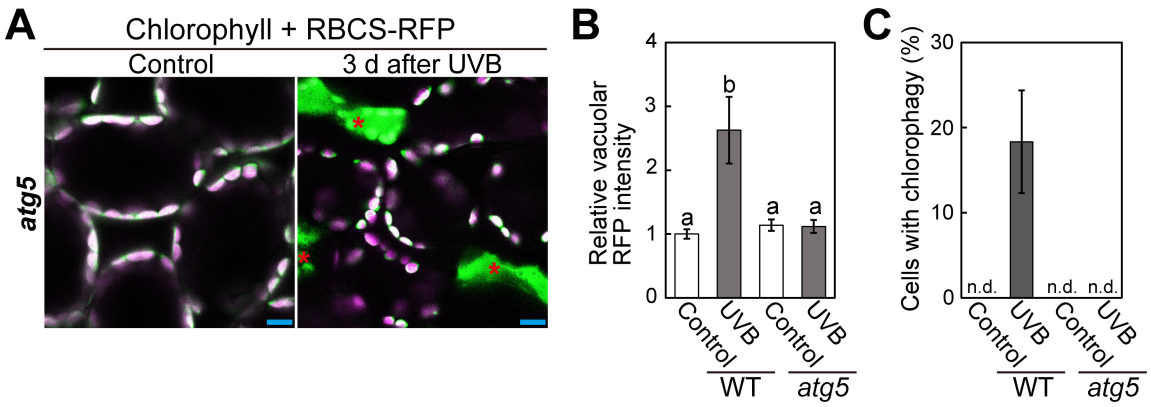

Supplemental Figure 7. The accumulation of vacuolar RFP in UVB-exposed leaves of *ProRBCS:RBCS-mRFP* plants is an autophagy-dependent phenomenon.

(A) Confocal images of mesophyll cells expressing stromal RBCS-mRFP from untreated control leaves or leaves exposed to UVB (1.5 W m^{-2}) for 2 h. Images were taken 3 d after treatment in wild-type and *atg5* mutant plants. Chlorophyll appears magenta and RFP appears green; merged images are shown. Scale bars = 10 μm. Asterisks denote dead cells.

(B) and **(C)** Quantification of the vacuolar RFP intensity and chlorophagy appearance 3 d after treatment from observations described in (**A)** (±SE, *n* = 3-4). Vacuolar RFP intensity is shown as relative to the data of WT control leaves, which is represented as 1. As the indicator of chlorophagy, the proportion of the cells containing vacuolar RBCS-RFP-deficient chloroplasts in a fixed region (212 × 212 × 40 μm each) was measured. Vacuolar RBCS-RFP-deficient chloroplasts were not detected (n. d.) in control WT plants and *atg5* plants. Different letters denote significant differences from each other based on Tukey's test (P< 0.05).

(Supports Figure 9.)

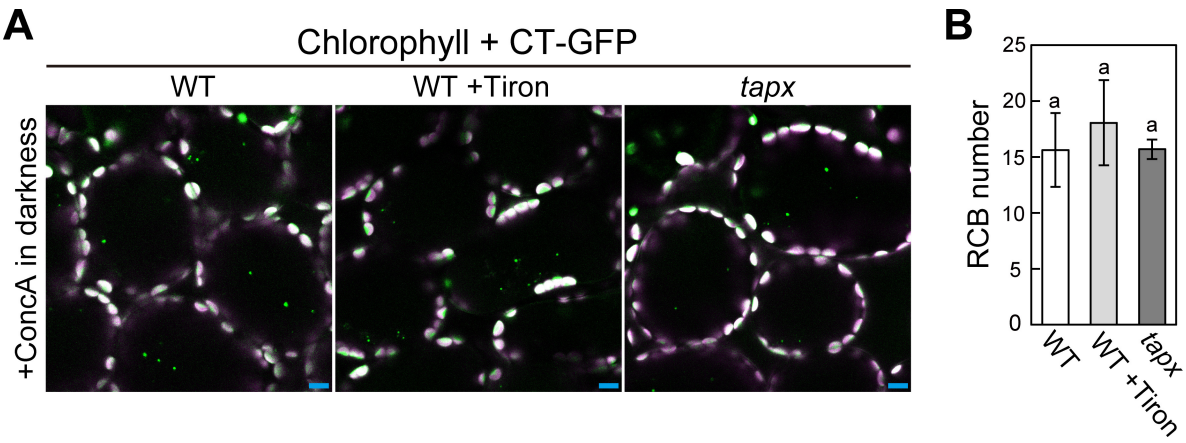

Supplemental Figure 8. RCB production is not affected by the presence of a scavenger of O_2^- or the knockout mutation of *tAPX*.
(A) Confocal images of mesophyll cells expressing stromal CT-GFP after a 20-h incubation with ConcA in darkness. 3rd rosette leaves from 25-d-old WT or *tapx* mutant plants were excised and incubated in 10 mM MES-NaOH (pH 5.5) containing 1 μM ConcA with or without 50 mM Tiron for 20 h in darkness. Chlorophyll appears magenta and CT-GFP appears green; merged images are shown. Small vesicles of 1-μm diameter exhibiting GFP are RCBs. Scale bars =10 μm.

(Supports Figure 9.)

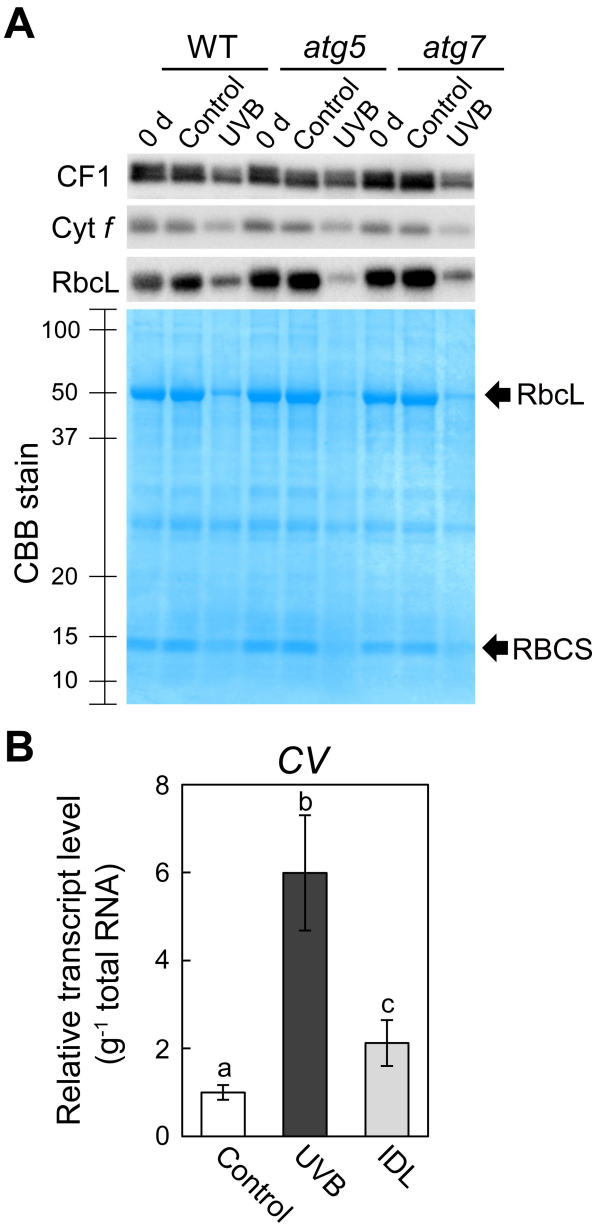

Supplemental Figure 9. The changes of chloroplast protein content in total leaf protein extracts after UVB damage does not reflect the impaired chlorophagy in *atg5* and *atg7*.
(A) Immunoblot detection of CF1, Cyt *f* and RbcL, and CBB stain in total protein extracts from leaves before treatment (0 d), untreated control leaves or 2-h UVB (1.5 W m^{-2})-exposed leaves 3 d after treatment in WT, *atg5* and *atg7* plants. Total protein extract from leaves of equal fresh weight were loaded. Sizes of molecular mass markers (kD) are indicated on the left of the stained gel.
(B) The transcript level of *CV* in samples described in Supplemental Figure 6C (±SE, *n* = 3-4). Transcript levels are shown as relative to the values of control leaves, which are represented as 1. Different letters denote significant differences from each other based on Tukey's test (P< 0.05).

(Supports Figure 9.)

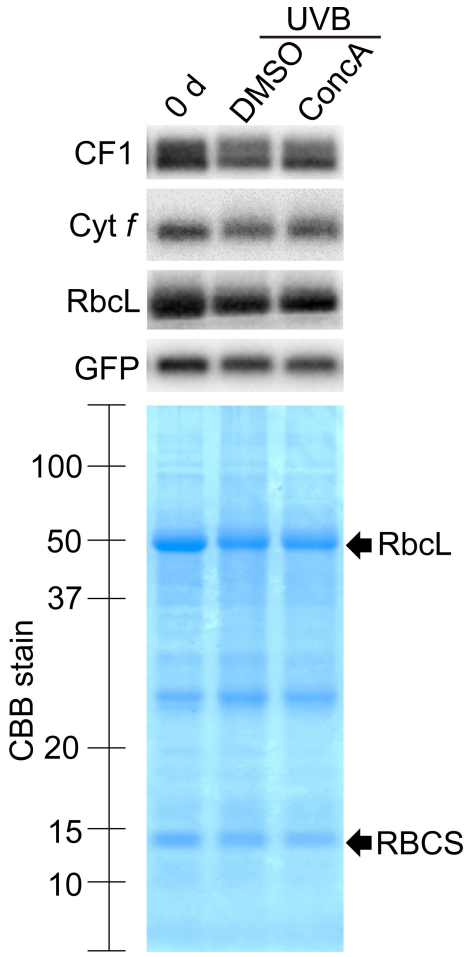

Supplemental Figure 10. Chloroplast protein abundance in UVB-damaged leaves after incubation with or without ConcA, an inhibitor of vacuolar lytic activity.
Immunoblot detection of CF1, Cyt f , RbcL and stroma-targeted GFP, and CBB stain in total protein extracts from leaves expressing CT-GFP before treatment (0 d) or 2 d after a 2-h UVB treatment at 1.5 W m^{-2}. UVB-exposed leaves 1 d after treatment were incubated for 20 h without (DMSO) or with ConcA. Equal amounts of protein were loaded. Sizes of molecular mass markers (kD) are indicated on the left of the stained gel.

(Supports Figure 9.)

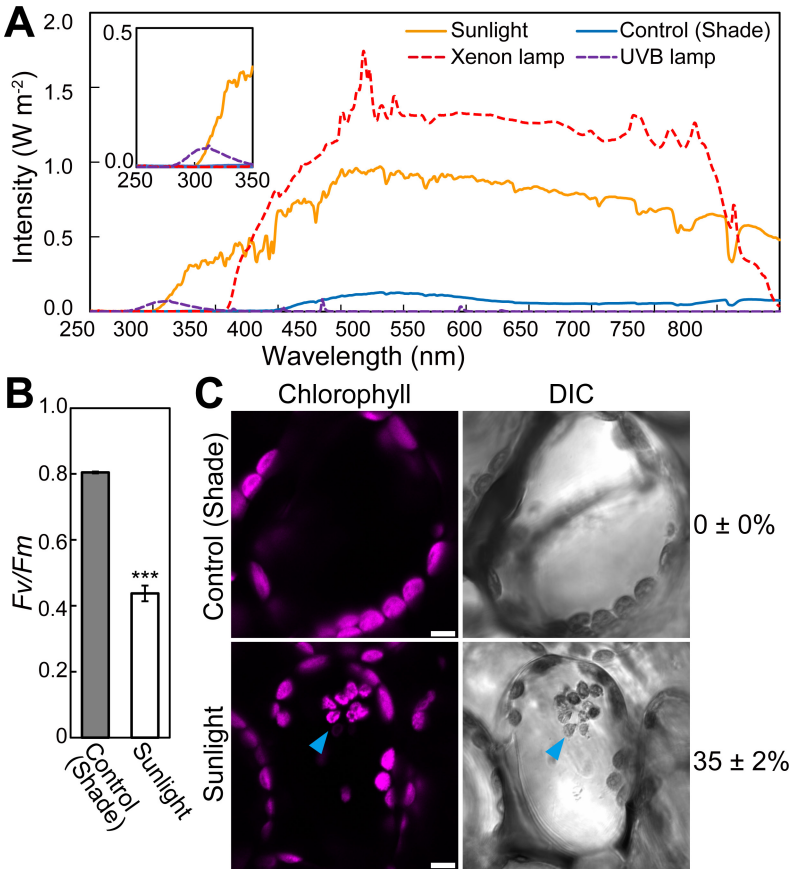

Supplemental Figure 11. Activation of chlorophagy by natural sunlight-induced damage.
(A) The spectra between 250 and 800 nm of natural sunlight and shaded natural sunlight as a control. The average of four measurements during 3-h irradiation are shown. The intensity of UVB and PAR measured with a data logger equipped with a UVB sensor or PAR sensor were 1.6-2.7 W m^{-2} and 900-1600 µmol $m^{-2}s^{-1}$ in sunlight or 0.01-0.02 W m^{-2} and 115-200 µmol $m^{-2}s^{-1}$ under the control (shaded) conditions, respectively. The spectra of the UVB lamp and Xenon light correspond to 1.5 W m^{-2}-UVB in Figure 2 and 2000 µmol $m^{-2}s^{-1}$-visible light in Figure 10, respectively.
(**B**) The *Fv/Fm* ratio in shaded control leaves or 3-h natural sunlight-irradiated leaves (±SE, *n* = 4). Asterisk denotes significant difference between conditions based on *t* test (***P<0.001).
(**C**) Confocal images of a leaf mesophyll cell from shaded control plants or plants exposed to natural sunlight for 3 h. Images were taken 2 d after treatment. Chlorophyll autofluorescence and DIC images are shown. Arrows indicate vacuolar chloroplasts. Scale bars = 10 µm. Values represent the proportion of cells containing vacuolar chloroplasts within a fixed area (±SE, *n* = 4).

(Supports Figure 10.)

Supplemental Table 1. The Sequences of Primers for Gene Cloning or qRT-PCR Analysis.

Gene (Locus)	Primer sequence (5' to 3')		Amplicon size (bp)	Reference
	Forward	Reverse		
OEP7 (At3g52420)	CACCATGGGAAAAACTTCG	CAAACCCTCTTTGGATGTGG	196	This study
18S rRNA	AATTGTTGGTCTTCAACGAGGAA	AAAGGGCAGGGACGTAGTCAA	74	1
DIN6 (At3g47340)	AACTTGTCGCCAGATCAAGG	GGAACACGTGCCTCTAGTCC	90	2
DIN1 (At4g35770)	GGCGATCACAGACATTGCTG	AGCTCATTCTCTGTCCAAGCG	52	3
DIN10 (At5g20250)	GATTCTTCGTGCTCGACTCC	TTAGCAAGCTGACACCATCAC	84	2
APX1 (At1g07890)	TGCCTTTTTCGCTGATTACG	CAAAAACAGCCATGACTCTCG	127	4
At4g10500	GTCCGAGGTCGAGAGTTCTG	CGCACTAGCAAGTTGTTGGA	100	5
At1g49150	GACACGACGCCTACAGACAA	CAACATCTCCATCGCATCAG	84	5
TH8 (At1g69880)	TTAATGAGCGTGTGGATGGA	TCACACCCACAACCATGTCT	94	5
CV (At2G25625)	CGGAGGTGGAGTGACAAGAG	GAGCAGACGGACGAGGAAGA	91	6
tAPX (At1g77490)	CAGAATGGGACTTGATGACAAGGAAA	ATGCAGCCACATCTTCAGCATACTTC	299	7

[1]Izumi et al., 2012 [2]Baena-González et al., 2007 [3]Carbonell-Bejerano et al., 2010 [4]Shao et al., 2013 [5]Ramel et al., 2012 [6]Wang and Blumward, 2014 [7]Maruta et al., 2012